Molecular Cell, Vol. 19, 53–63, July 1, 2005, Copyright ©2005 by Elsevier Inc. DOI 10.1016/j.molcel.2005.05.007

Cotranscriptional Spliceosome Assembly Occurs in a Stepwise Fashion and Requires the Cap Binding Complex

Janina Görnemann, Kimberly M. Kotovic, Katja Hujer, and Karla M. Neugebauer*
Max Planck Institute of Molecular Cell Biology and Genetics
Pfotenhauerstrasse 108
01307 Dresden
Germany

Summary

Coupling between transcription and pre-mRNA splicing is a key regulatory mechanism in gene expression. Here, we investigate cotranscriptional spliceosome assembly in yeast, using in vivo crosslinking to determine the distribution of spliceosome components along intron-containing genes. Accumulation of the U1, U2, and U5 small nuclear ribonucleoprotein particles (snRNPs) and the 3′ splice site binding factors Mud2p and BBP was detected in patterns indicative of progressive and complete spliceosome assembly; recruitment of the nineteen complex (NTC) component Prp19p suggests that splicing catalysis is also cotranscriptional. The separate dynamics of the U1, U2, and U5 snRNPs are consistent with stepwise recruitment of individual snRNPs rather than a preformed "penta-snRNP," as recently proposed. Finally, we show that the cap binding complex (CBC) is necessary, but not sufficient, for cotranscriptional spliceosome assembly. Thus, the demonstration of an essential link between CBC and spliceosome assembly in vivo indicates that 5′ end capping couples pre-mRNA splicing to transcription.

Introduction

Pre-mRNA splicing is carried out by the spliceosome, a multicomponent complex approximately the size of the ribosome (Jurica and Moore, 2003; Nilsen, 2003). The two-step *trans*-esterification reaction, which leads to cleavage of the RNA at intron-exon boundaries and the ligation together of two adjacent exons, depends upon the sequential activities of the spliceosomal small nuclear RNAs (snRNAs) U2, U4, U5, and U6. Prior to splicing, recognition of the 5′ and 3′ splice sites by the U1 and U2 snRNAs, augmented by snRNP and non-snRNP splicing factors, serves to define the splice sites and to stimulate spliceosome assembly. Transitions from splice site recognition to the initiation of splicing and during catalysis are marked by profound rearrangements in snRNA-pre-mRNA and snRNA-snRNA base-pairing interactions (Staley and Guthrie, 1998). Whether these dynamics are carried out within a preformed spliceosomal machine or whether they reflect the addition and loss of individual spliceosomal components bound to the pre-mRNA is an unresolved question.

*Correspondence: neugebau@mpi-cbg.de

Until recently, it has been assumed that spliceosome assembly occurs in a step-wise fashion, with the U1 snRNP and the U2 snRNP added independently to pre-mRNA, followed by the addition of the U4/U6•U5 tri-snRNP (Reed, 2000). The U1, U2, and U4/U6•U5 tri-snRNPs can be isolated individually from nuclear extracts, which are capable of splicing pre-mRNA in the presence of ATP. Moreover, distinct intermediates in spliceosome assembly can be detected and purified. In yeast and mammals, early ATP-independent assembly steps include the formation of commitment or E complexes, reflecting pre-mRNA association with the U1 snRNP and the 3′ splice site factors BBP (SF1 in mammals) and Mud2p (U2AF65 in mammals) (Abovich and Rosbash, 1997; Michaud and Reed, 1991; Seraphin and Rosbash, 1989). After the addition of ATP to in vitro splicing reactions, the U2 snRNP joins to form mammalian complex A, and further separable steps in spliceosome assembly can be arrested (Chiara et al., 1996). Purification of these complexes in biochemical amounts has permitted their proteomic characterization by mass spectrometry, providing a detailed list of proteins that participate in the splicing reaction (Jurica et al., 2002; Makarov et al., 2002; Rappsilber et al., 2002; Zhou et al., 2002).

However, it has recently been shown in yeast that, depending on the salt concentration used in preparing the nuclear extract, a larger 45S particle containing all of the spliceosomal snRNPs is present (Stevens et al., 2002). This has given rise to the penta-snRNP hypothesis, which holds that all five spliceosomal snRNPs are recruited to pre-mRNA together; within this super complex of pre-mRNA and spliceosomal components, all of the aforementioned dynamics between pre-mRNA and snRNAs may take place. Support for the penta-snRNP hypothesis has come from in vitro evidence in higher eukaryotes that the U1 and U5 snRNPs contact the 5′ splice site independently of 3′ splice site recognition and/or in the context of a mammalian penta-snRNP (Malca et al., 2003; Maroney et al., 2000; Wyatt et al., 1992). Moreover, it has long been known that large 200S complexes, containing all of the spliceosomal snRNPs, most non-snRNP splicing factors, and pre-mRNA, can be isolated by gradient centrifugation of HeLa nuclear extracts (Miriami et al., 1995; Raitskin et al., 2002). This mammalian complex, now termed the supraspliceosome, may accommodate multiple penta-snRNPs (Azubel et al., 2004). This body of data has called into question the composition of the spliceosomal machine and its parts (Nilsen, 2002; Nilsen, 2003).

How do spliceosomes assemble in vivo? Until recently, this question has been difficult to address. Results from metazoan systems indicate that splicing at least begins cotranscriptionally (Neugebauer, 2002), raising the possibility that spliceosome assembly can be monitored in vivo by examining the association of splicing factors along the lengths of genes. Because nascent RNPs lie adjacent to the DNA axis (Wetterberg et al., 2001), the use of formaldehyde to efficiently induce protein-protein and protein-nucleic acid cross-

links among nearby (~2 Å) reactive groups (Orlando, 2000) can potentially capture spliceosome assembly events that occur cotranscriptionally. Indeed, we found in previous work that cotranscriptional association of the U1 snRNP with intron-containing genes in *Saccharomyces cerevisiae* was detectable by chromatin immunoprecipitation (ChIP), in which cells are subjected to formaldehyde crosslinking prior to cell lysis, DNA shearing, immunoprecipitation, and PCR detection of purified DNA fragments (Kotovic et al., 2003). Thus, the ChIP approach offers the possibility of monitoring further events in spliceosome assembly with spatial and, by inference, temporal resolution, as nascent RNA is synthesized by RNA polymerase II (pol II) from the beginning to the end of the gene.

Here, we show by epitope-tagging endogenous genes encoding components of the U2 and U5 snRNPs, the NTC involved in spliceosome activation, and the 3′ splice site factors Mud2p and BBP (branchpoint binding protein) that spliceosome assembly proceeds to apparent completion by the time RNA pol II has reached the end of intron-containing genes. Moreover, the distinct patterns of accumulation observed indicate that individual components of the spliceosome are recruited in a step-wise fashion. Because 5′ end capping of mRNAs also occurs cotranscriptionally (Shuman, 2001), and because the nuclear CBC binds the cap cotranscriptionally and is thought to stimulate splicing (Dower and Rosbash, 2002; Izaurralde et al., 1994; Le Hir et al., 2003; Visa et al., 1996; Zenklusen et al., 2002), cotranscriptional spliceosome assembly was examined in a strain bearing viable deletions of both subunits of CBC (CBP20 and CBP80). Two opposing models for CBC function in splicing have been proposed: (1) that CBC may promote early steps in splicing, such as commitment complex formation and/or U1 snRNP recruitment (Abovich et al., 1994; Colot et al., 1996; Fortes et al., 1999a; Fortes et al., 1999b; Lewis et al., 1996a; Lewis et al., 1996b), or (2) that CBC may facilitate removal the U1 snRNP by the helicase Prp28 upon association of the tri-snRNP (Chen et al., 2001; O'Mullane and Eperon, 1998). We provide evidence for both of these roles of CBC, which are differentially detected on the genes under study. On every gene examined here, U5 snRNP accumulation was nearly abolished, indicating that CBC is required for proper coupling of splicing to transcription in yeast.

Results

As a first step toward examining cotranscriptional spliceosome assembly, we asked whether the commitment complex components Mud2p, BBP, and the U2 snRNP were detectable on intron-containing genes by ChIP. Strains were created in which the endogenous genes encoding Mud2p, BBP, and the U2 snRNP-specific proteins Lea1p and Msl1p were epitope tagged in an otherwise wild-type (wt) background. ChIP was performed with tag-specific monoclonal antibodies (mAbs) and with 8WG16 specific for RNA pol II as a positive control and internal reference; immunopurified DNA was detected and quantified by real-time PCR. Figure 1 shows that all of the tagged commitment complex components were detectable on two endogenous intron-containing genes, *ECM33* and *DBP2-GFP*, in which the *DBP2* gene was lengthened by tagging the *DBP2* ORF with the green fluorescent protein (730 bp). These genes differ in their structure and therefore provide different sets of information (see gene diagrams in Figure 1). *DBP2* has a very long first exon (1273 bp) and long intron (1003 bp), facilitating the separation of early events in splicing factor recruitment from pol II accumulation at the promoter. In contrast, *ECM33* has a short first exon and short intron, whereas the long second exon (1348 bp) provides additional resolution in downstream regions.

The distributions of Mud2p and BBP, which bind directly to 3′ splice site intronic elements (the polypyrimidine tract and branchpoint, respectively) were identical, reaching maximum signals over gene regions that coincided with the accumulation of the U1 snRNP (Figure 1, top four panels). Interestingly, the observed peak on *DBP2* precedes somewhat the position of the branchpoint sequence, suggesting that either or both of these proteins may interact with additional intronic sequences in this pre-mRNA. Note that ChIP signals with tagged Prp42p, one component of the U1 snRNP, were previously shown to coincide with other tagged components of the U1 snRNP, establishing that Prp42p detection is indicative of intact U1 snRNP accumulation (Kotovic et al., 2003). In *DBP2-GFP*, the U1 snRNP, Mud2p, and BBP were enriched 5-fold over promoter levels at a position corresponding to the middle of the intron, whereas each of these factors was enriched ~20-fold at the *ECM33* 3′ splice site as compared to a region 500 bp upstream of the promoter. U1 snRNP, Mud2p, and BBP declined in downstream regions, returning to very low levels in downstream regions of both *DBP2-GFP* and *ECM33*. The distribution of each of these factors on *SAC6*, a gene with similar intron/exon structure to *ECM33*, was similar to that shown for *ECM33* (data not shown). We conclude from this that U1 snRNP, Mud2p, and BBP accumulate cotranscriptionally in identical patterns, suggesting that their correlated appearance on intron-containing genes represents commitment complex formation.

The U2 snRNP was also detectable cotranscriptionally but accumulated in a pattern distinct from U1 snRNP, Mud2p, and BBP (Figure 1, lower two panels). Tagged Lea1p and Msl1p proteins yielded identical results, indicating that the intact U2 snRNP was detected. On *DBP2-GFP*, the ChIP signals for both proteins peaked 200 bp downstream of the 3′ splice site, 1 kb after the peak of the U1 snRNP, Mud2p, and BBP. On *ECM33*, the U2 snRNP was detected in a broad peak, beginning 100 bp downstream of the 3′ splice site and initially overlapping with the U1 snRNP, Mud2p, and BBP; this overlap is expected, because the *ECM33* intron is only 331 bp long. However, in contrast to these earlier factors, U2 snRNP levels remained high in regions downstream of their initial peak on *DBP2-GFP*, *ECM33*, and *SAC6* (data not shown). This indicates that the decrease in U1 snRNP, Mud2p, and BBP detection is not a general phenomenon of decreased accessibility in downstream gene regions. Taken together, these data indicate that U2 snRNP concentrates on intron-

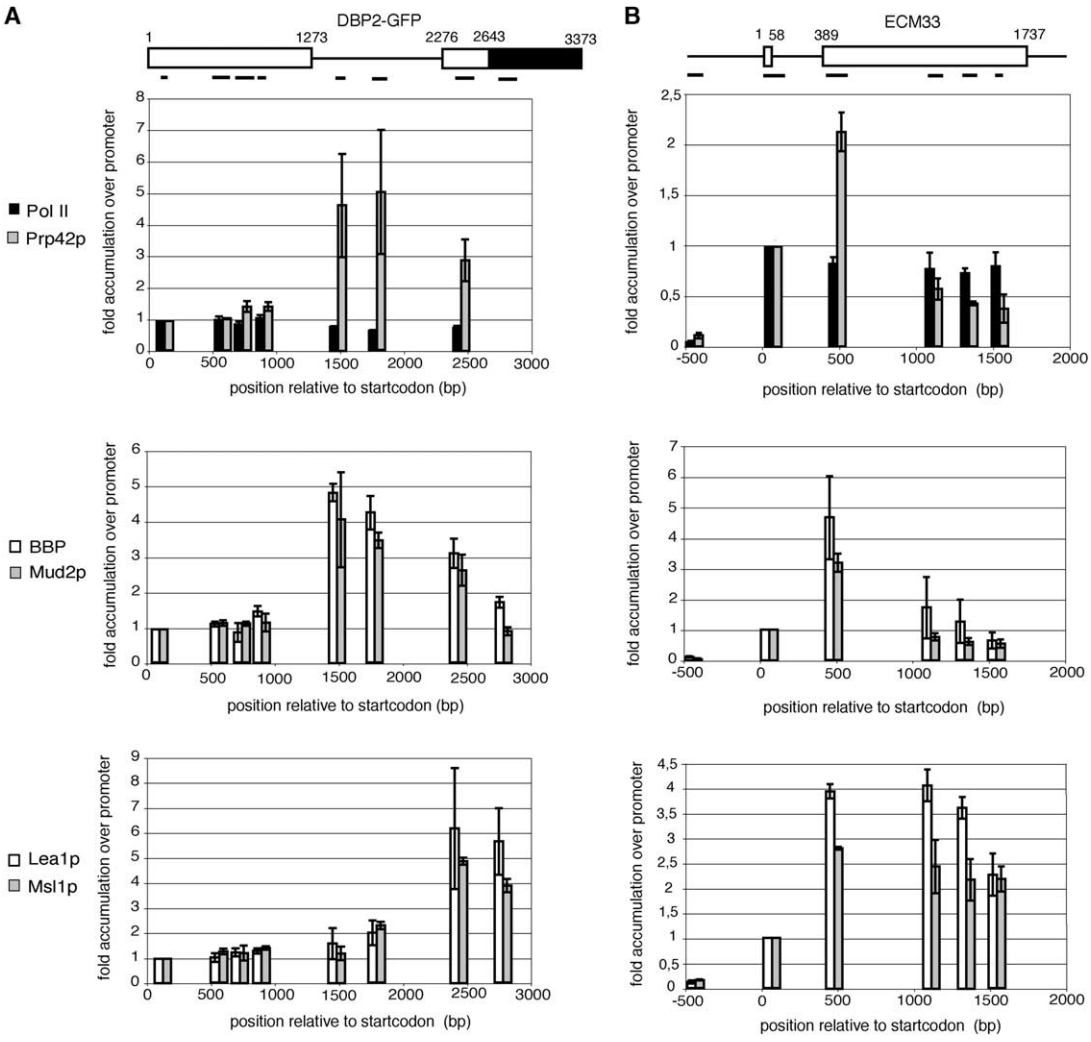

Figure 1. Cotranscriptional Commitment Complex Formation and U2 snRNP Addition

Diagrams representing the genes *DBP2-GFP* (A) and *ECM33* (B) show the positions of the PCR products used for analysis. In the panels aligned immediately below these diagrams, histogram bars are placed according to the positions of the PCR products along each gene. Error bars represent the SD.

(A) Whereas the amount of RNA pol II remains constant along *DBP2-GFP*, the dynamics of splicing factor association can be observed. Components of the commitment complex (PrP42p in the U1 snRNP, BBP, and Mud2p) accumulate after synthesis of the 5′ splice site, and U2 snRNP factors (Lea1p and Ms11p) can be detected after synthesis of the 3′ splice site. The levels of accumulation of the analyzed factors are expressed relative to the promoter-proximal position.

(B) Compared to an upstream position (–500 bp), RNA polymerase II (pol II) levels increase 20-fold and remain constant along *ECM33*. In contrast, splicing factors increase compared to promoter levels after synthesis of the splice sites as in (A).

The data represent the average of at least three independent experiments. (A) Prp42p, n = 3; BBP, n = 4; Mud2p, n = 6; Lea1p, n = 3; and Msl1p, n = 3. (B) Prp42p, n = 3; BBP, n = 4; Mud2p, n = 5; Lea1p, n = 3; Msl1p, n = 3.

containing genes after 3′ splice site synthesis and persists after detectability of U1 snRNP, Mud2p, and BBP has been lost. Thus, U1 and U2 snRNP dynamics are distinct with respect to each other and with respect to their position along intron-containing genes.

To extend these results to later steps in spliceosome assembly, we tagged endogenous genes encoding three components of the U5 snRNP (Prp8p, Brr2p, and Snu114p). In this context, we assume the U5 snRNP marks the arrival of the U4/U6•U5 tri-snRNP and potentially remains until catalysis; due to the fact that the U4/U6 snRNP disassembles upon tri-snRNP addition to the spliceosome, we did not choose any U4/U6 snRNP proteins for tagging. Instead, we tagged Prp19p, one of ~11 proteins comprising the NTC that associates with the spliceosome after tri-snRNP addition and is thought to activate the spliceosome for catalysis (Chan et al., 2003; Makarova et al., 2004; Ohi et al., 2005; Tarn et al., 1994). Figure 2 shows that all four of these tagged proteins accumulate cotranscriptionally. On *DBP2-GFP*, all three U5 snRNP components and Prp19p peaked at the most downstream position examined, ~500 bp after the 3′ splice site, reaching levels ~10-fold (Brr2p and Snu114p), ~8-fold (Prp8p), and ~15-fold (Prp19p) above promoter levels. On *ECM33*, all four proteins reached their peak signals (~20-fold over upstream)

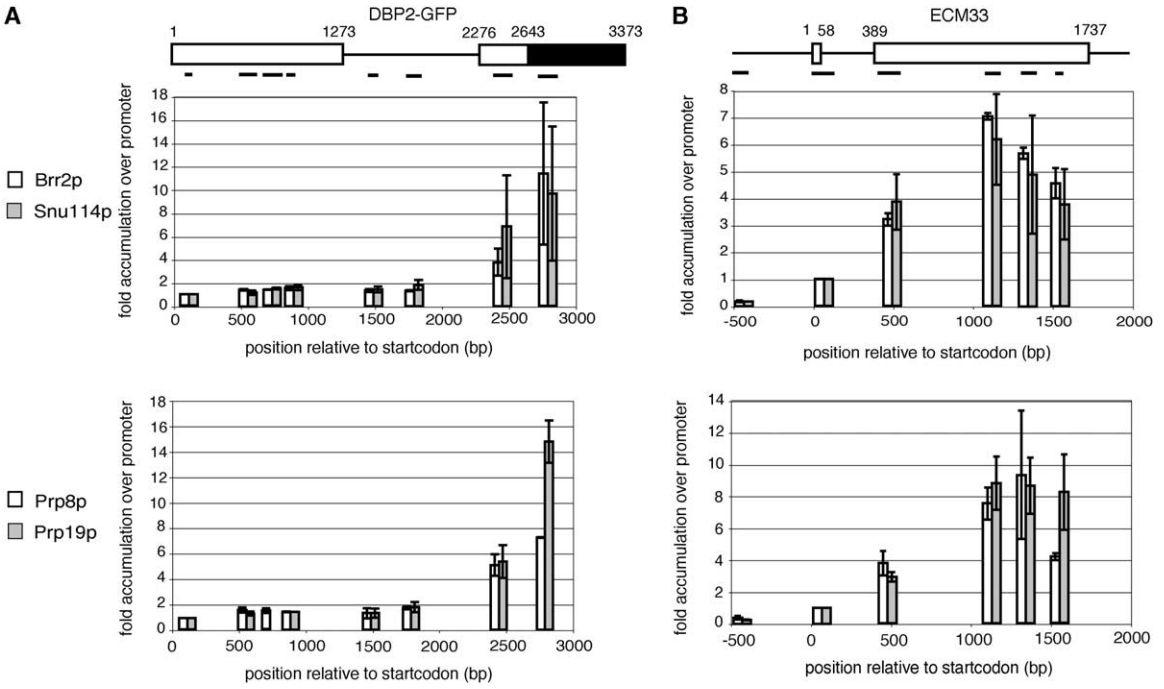

Figure 2. Cotranscriptional Formation of the Active Spliceosome

Levels of U5 snRNP components (Brr2p, Snu114p, and Prp8p) and NTC component Prp19p increase strongly downstream of the 3′ splice site on *DBP2-GFP* (A) and *ECM33* (B). The setup of the figure is the same as in Figure 1. Values were normalized by setting the promoter-proximal position to 1. The data represent the average of three independent experiments, except in (B), Prp8 (n = 4). Error bars represent the SD.

800 bp after 3′ splice site synthesis. Thus, U5 snRNP and Prp19p accumulation is inversely related to U1 snRNP accumulation (see Figure 1), consistent with evidence that the U1 snRNP must leave the pre-mRNA upon tri-snRNP recruitment and before spliceosome activation (Konforti et al., 1993; Makarov et al., 2002). The robust detection of Prp19p further suggests that assembly of catalytically competent spliceosomes is completed during ongoing transcription.

To facilitate a direct comparison of the recruitment dynamics of each of the snRNPs examined, the data presented in Figures 1 and 2 were plotted to show the percent of maximum signal with respect to position along the *DBP2-GFP* and *ECM33* genes (Figure 3). Note that although BBP and Mud2p were excluded from the plot, their distribution was identical to the U1 snRNP (see Figure 1). Both graphs show that the patterns of the U1 snRNP, the U2 snRNP, and the U5 snRNP are clearly distinct from one another. On *DBP2-GFP*, the onset of accumulation of each snRNP is resolved, with the U1 snRNP peaking after 5′ splice site synthesis, the U2 snRNP after 3′ splice site synthesis, and the U5 snRNP still further downstream. On both *DBP2-GFP* and *ECM33*, the loss of the U1 snRNP is coincident with the arrival of the U5 snRNP. On *ECM33*, the distinction between U2 and U5 snRNP accumulation is made clear by the prolonged detection of U2 prior to the arrival of U5. Moreover, the distinct patterns of U1, U2, and U5 snRNP accumulation were also observed when all steps of the ChIP were carried out in 50 mM salt conditions (data not shown), which permit detection of the penta-snRNP in uncrosslinked extracts (Stevens et al., 2002); therefore, it is unlikely that the penta-snRNP was not detected due to incomplete crosslinking of the nascent RNP. These data do not support the penta-snRNP model of spliceosome assembly in which all five of the spliceosomal snRNPs are recruited together (Malca et al., 2003; Stevens et al., 2002). Instead, the data recapitulate the expectations of a stepwise recruitment model in which the spliceosomal snRNPs independently associate with nascent pre-mRNA elements during the natural course of transcription.

The nuclear CBC is detectable by ChIP in promoter-proximal regions of intron-containing as well as intronless genes (Zenklusen et al., 2002; data not shown); thus, CBC could potentially play a role in early and/or late steps of spliceosome assembly. We carried out our assay in a viable strain lacking both CBC subunits, CBP20 and CBP80 (Fortes et al., 1999a); any change in cotranscriptional spliceosome assembly must represent steady-state effects of CBC deletion. Components of the U1 snRNP (Prp42p), the U2 snRNP (Lea1p and Msl1p), and the U5 snRNP (Prp8p and Brr2p) as well as BBP and Mud2p were epitope tagged in ΔCBC and wt strains. Figure 4 shows clearly that CBC deletion completely abolished cotranscriptional spliceosome assembly on *DBP2*. U1 snRNP, U2 snRNP, U5 snRNP, and BBP levels were similar to background. Interestingly, Mud2p detection and pattern of distribution along *DBP2* were indistinguishable from wt, suggesting that

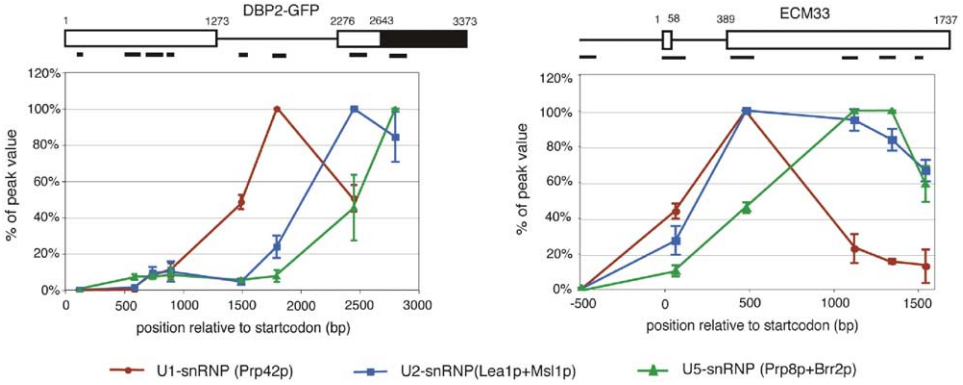

Figure 3. Sequential Accumulation of the U1, U2, and U5 snRNPs on *DBP2-GFP* and *ECM33*

When summarized in one diagram, the data from Figures 1 and 2 show that accumulation of the U1 (red line), U2 (blue line), and U5 (green line) snRNPs can be detected at different positions along the transcription unit. Along *DBP2-GFP* (left), the three factors accumulate and peak sequentially. Along *ECM33* (right), the U1 and the U2 snRNP distributions differ in downstream regions, and the pattern of U5 snRNP accumulation can be distinguished from both the U1 and U2 snRNPs. The peak value for each data set was set as 100%, the lowest as 0%. For the U2 snRNP data, Lea1p and Msl1p data were combined; for the U5 snRNP, Prp8p and Brr2p data were combined. Error bars represent the variation within data sets after this transformation.

the *DBP2* mRNA is transcribed at normal levels in the deletion strain and that the nascent RNA is at least partially available for binding to splicing factors. Consistent with this interpretation, quantitative RT-PCR detection of spliced and unspliced *DBP2* RNAs indicated that overall *DBP2* expression and splicing in the ΔCBC strain is similar to wt (Table S1 available in the Supplemental Data with this article online). This implies that *DBP2* pre-mRNA is posttranscriptionally spliced. Expression of CBP20 and CBP80 in the ΔCBC strain was sufficient to rescue U1 and U5 snRNP accumulation on *DBP2*, indicating that the cotranscriptional spliceosome assembly phenotypes observed are attributable solely to the loss of the CBC subunits (Figure 4). These data provide direct evidence that CBC is required for cotranscriptional accumulation of the U1 snRNP and BBP on *DBP2*, consistent with previous observations that CBC is a commitment complex component possibly required for U1 snRNP recruitment (Colot et al., 1996; Fortes et al., 1999a; Fortes et al., 1999b; Lewis et al., 1996a; Lewis et al., 1996b). The loss of U2 and U5 snRNP recruitment likely reflects the indirect effect of failure to recruit these early-acting factors.

Surprisingly, CBC deletion produced a different spliceosome assembly phenotype on seven other genes examined. On *ECM33* (Figure 5), *ASC1*, and *SAC6* (data not shown), U5 snRNP accumulation was nearly undetectable; however, the accumulation and distribution of BBP, Mud2p, and the U2 snRNP in ΔCBC cells were identical to wt. Strikingly, U1 snRNP accumulation persisted in downstream regions (4-fold above wt levels) when CBC was deleted. The wt distributions of U1 and U5 snRNPs were restored upon induced expression of both CBC subunits. Consistent with these results, retention of the U1 snRNP and loss of U5 in ΔCBC cells was also observed on *RPS9A*, *RPS9B*, *RPS11A*, and *RPS11B* genes (data not shown); splicing of *RPS9A* and *RPS11B* pre-mRNAs was shown to be blocked in this ΔCBC strain (Fortes et al., 1999b). Thus, on these seven genes, the CBC is not required for commitment complex formation, yet CBC is required for the normal loss of the U1 snRNP and the appearance of the U5 snRNP in downstream gene regions. In contrast to the results obtained on *DBP2*, these data support the proposal that CBC promotes the release of the U1 snRNP and the subsequent association of the tri-snRNP (O'Mullane and Eperon, 1998).

Because CBC was required for proper cotranscriptional spliceosome assembly on all intron-containing genes examined, we tested whether CBC was sufficient for splicing factor accumulation on an intronless pol II gene. For this analysis, three positions within the 4536 bp-long *PDR5* gene and one position 500 bp upstream of the promoter were examined. Although pol II was detectable at the promoter (10-fold relative to upstream) and downstream regions of *PDR5* (~6-fold), the U1 snRNP, BBP, the U2 snRNP, the U5 snRNP, and Prp19p were poorly detected at the *PDR5* promoter and downstream regions in both wt and ΔCBC strains (Figure 6). In contrast, Mud2p was detectable in *PDR5* gene regions ~4-fold above the upstream region. Thus, Mud2p may associate to some significant extent with pol II and/or all nascent mRNAs, consistent with the proposed role of the metazoan Mud2p homolog U2AF in nuclear export of intronless mRNAs (Blanchette et al., 2004; Ujvari and Luse, 2004). Further concentration of Mud2p in downstream regions has only been observed in intron-containing genes, confirming that accumulation of Mud2p on the *DBP2* gene in the absence of CBC is most likely due to nascent RNA binding (see Figure 4). Finally, CBC deletion did not alter the detectability of any splicing factor on *PDR5*, indicating that CBC alone is not sufficient for any aspect of cotranscriptional spliceosome assembly examined here.

Discussion

Here, we have mapped the positions at which spliceosomal components accumulate cotranscriptionally

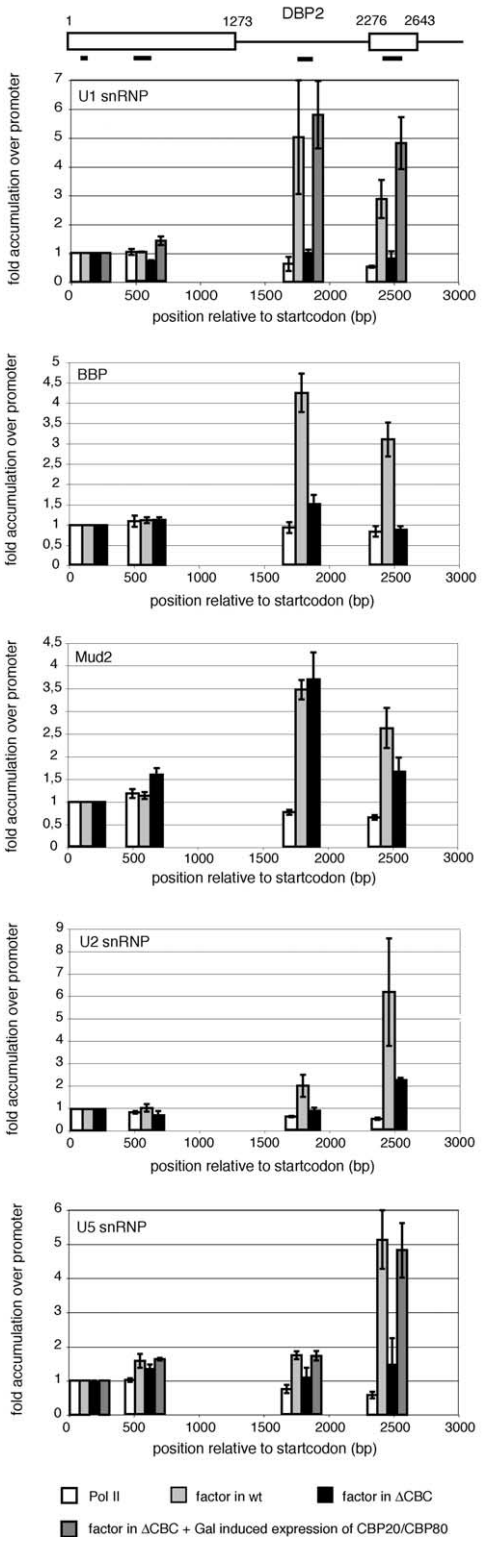

Figure 4. Evidence that the CBC Is Required for Commitment Complex Formation on *DBP2*

Direct comparison between the levels of splicing factors detected on *DBP2* in wt and ΔCBC mutant strains. Loss of detection is evident in the ΔCBC mutant strain for the U1 snRNP (Prp42p), BBP, the U2 snRNP (Lea1p), and the U5 snRNP (Prp8p), but not for Mud2p. Galactose-induced expression of CBP20 and CBP80 rescues the U1 snRNP (Prp42p) and U5 snRNP (Prp8p and Brr2p) distributions, top and bottom panels, respectively (n = 2 in each). For the U2 snRNP and the U5 snRNP, results with Msl1p and Brr2p were indistinguishable from those shown. The distribution of pol II was the same in wt and the ΔCBC strain with respect to the promoter-proximal position. ΔCBC data sets represent the average of U1 snRNP, n = 3; BBP, n = 5; Mud2p, n = 4; U2 snRNP, n = 3; and U5 snRNP, n = 8 independent experiments. Error bars indicate SD.

within intron-containing genes in yeast. This was made possible by ChIP of tagged versions of U1, U2, and U5 snRNP-specific factors as well as the 3′ splice site factors BBP and Mud2p and a component of the nineteen complex (Prp19p) involved in spliceosome activation. Making use of primer sets that distinguish between gene regions, we found that these components segregate spatially along the length of genes, falling into three separable patterns of accumulation. The first group of factors to associate with intron-containing genes comprises the U1 snRNP, BBP, and Mud2p, which peak following 5′ splice site synthesis and later decline; this event is interpreted as commitment complex formation and precedes the accumulation of the U2 snRNP, which occurs shortly after 3′ splice site synthesis. The U2 snRNP, in contrast to the commitment complex group, remains high in downstream gene regions and overlaps with the third and latest group detected, the U5 snRNP and Prp19p. CBC deletion was shown to abolish proper U5 snRNP accumulation on every gene examined by two different mechanisms discussed below. Taken together, these observations lead to two overall conclusions, diagrammed in Figure 7: (1) that cotranscriptional spliceosome assembly proceeds via stepwise snRNP addition, with no evidence for the penta-snRNP model of assembly, and (2) that the CBC couples splicing to transcription in yeast.

The yeast penta-snRNP contains the U1, U2, U4, U5, and U6 snRNPs as well as many non-snRNP spliceosomal factors and can support pre-mRNA splicing in vitro; this observation raised the possibility that the snRNPs preassemble before interacting with pre-mRNA (Stevens et al., 2002). With respect to the cotranscriptional assembly of spliceosomes in yeast, the clear predictions of the two models are either (1) all of the snRNPs are recruited simultaneously in the case of the penta-snRNP model or (2) snRNPs are recruited individually in the case of the stepwise assembly model. The key observation is that the distributions of the U1, U2, and U5 snRNPs along every intron-containing gene examined here were distinguishable from one another (see Figure 3), even under low-salt conditions expected to preserve the penta-snRNP. On the *DBP2* gene, the U2 snRNP peaked ~1 kb after the peak of the U1 snRNP, and U2 snRNP levels remained high in downstream regions where the U1 snRNP declined. U1 and U2 snRNP distributions also differed in downstream regions of *ECM33* and *SAC6* genes. The U1 and U5 snRNP distributions were separated by more that 1 kb on both *DBP2* and *ECM33*, consistent with the results of Lacadie and Rosbash (2005, this issue of Molecular Cell). Separability of the U2 and U5 snRNP distributions can be appreciated by the 500–700 bp delay of U5 snRNP accumulation with respect to the U2 snRNP on *DBP2*

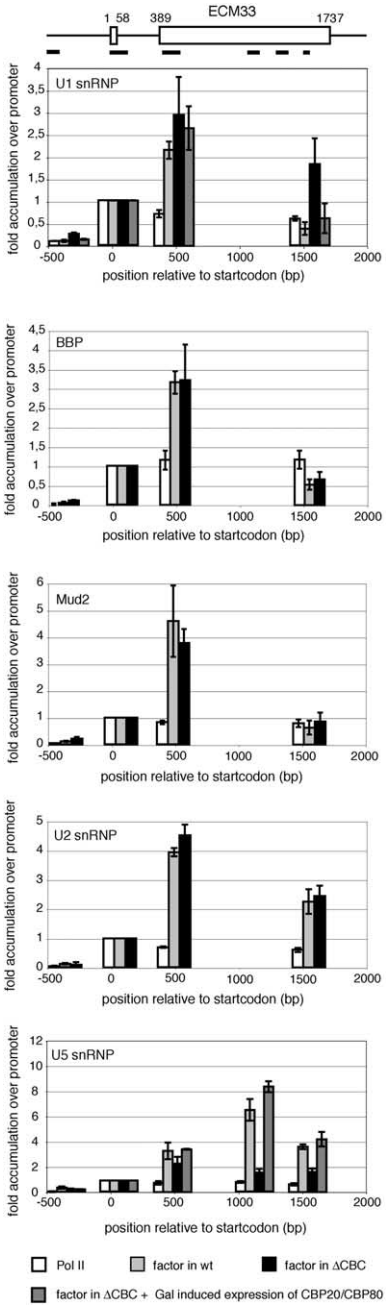

Figure 5. Evidence that the CBC Plays a Role in U1 snRNP Removal and U5 snRNP Accumulation on *ECM33*

Direct comparison between the levels of splicing factors detected on *ECM33* in wt and ΔCBC mutant strains. The levels and overall patterns of BBP, Mud2p, and the U2 snRNP accumulation were unaffected. Whereas the levels of U1 snRNP detected in the mutant were comparable to wt, U1 snRNP detection was prolonged in downstream regions. In contrast, levels of U5 snRNP accumulation are strongly reduced in the mutant. Galactose-induced expression of CBP20 and CBP80 rescues the U1 snRNP (Prp42p) and U5 snRNP (Prp8p and Brr2p) distributions, top and bottom panels, respectively (n = 2 in each). The U2 snRNP is represented by Lea1p; Msl1p gave identical results. For the U5 snRNP, Prp8p data are shown; Brr2p gave identical results. ΔCBC data sets represent the average of U1, n = 4; BBP, n = 3; Mud2p, n = 3; U2 snRNP, n = 3; and U5 snRNP, n = 3 independent experiments. Error bars indicate SD.

and *ECM33*. Finally, the loss of the U5 and retention of the U1 and U2 snRNPs upon CBC deletion (see below) further substantiate the independence of snRNP recruitment. Although we cannot completely exclude the formal possibility that the penta-snRNP is poorly detectable by the methods employed here, the fact that these data recapitulate the predictions of stepwise assembly in vivo leads us to favor this model, rather than the penta-snRNP model, as the mechanism of cotranscriptional spliceosome assembly.

Evidence accumulating from metazoan systems indicates that pre-mRNA splicing is cotranscriptional (Neugebauer, 2002). Although cotranscriptional pre-mRNA splicing has never been directly demonstrated in yeast, two previous studies are suggestive: in one, the kinetics of appearance of spliced mRNA were examined and favored concurrent splicing and transcription (Elliott and Rosbash, 1996), and in another, the U1 snRNP was shown to be cotranscriptionally recruited to intron-containing genes on a genome-wide scale (Kotovic et al., 2003). The data presented here on Prp19p further suggest that splicing can occur cotranscriptionally in yeast. Prp19p is the defining component of the NTC, which is required for U5 and U6 snRNP association with pre-mRNA after the U4 snRNP has left the spliceosome (Chan et al., 2003). This observation and the detection of NTC components in activated spliceosomes by mass spectrometry (Makarov et al., 2002) indicate that Prp19p is a marker of spliceosome activation. Thus, the observed accumulation of Prp19p on downstream gene regions, overlapping with the U5 snRNP distribution (see Figure 2), is a strong indication that spliceosome activation occurs cotranscriptionally in yeast. Because RNA pol II transcribes at a rate of 1–1.5 kb/minute (Zorio and Bentley, 2004), we can infer from the position of the U5 snRNP and Prp19p that spliceosome assembly is complete ~30 s (600 bp) after transcription of the *ECM33* and *DBP2* 3′ splice sites. Interestingly, these data compare favorably with estimates of the time it takes to assemble spliceosomes after 3′ splice site synthesis in *Drosophila* (Beyer and Osheim, 1988), suggesting that the dynamics and general mechanisms of cotranscriptional spliceosome assembly are conserved across species.

Addition of a 7-methyl guanosine cap to the 5′ ends of RNA pol II transcripts occurs shortly after transcription initiation in all eukaryotes (Shuman, 2001), and failure to cap leads to the accumulation of unspliced pre-mRNA (Burckin et al., 2005; Fresco and Buratowski, 1996; Schwer and Shuman, 1996). The cap is bound cotranscriptionally by the nuclear CBC, a heterodimer composed of CBP80 and CBP20 subunits (Visa et al., 1996; Zenklusen et al., 2002). Two studies in yeast show that CBC plays an important role in splicing in vivo. First, although CBC deletion is viable and most pre-mRNAs are spliced, the splicing of a subset of pre-mRNAs is drastically reduced (Colot et al., 1996; Fortes et al., 1999b). Second, splicing of uncapped T7 RNA polymerase transcripts is significantly reduced, and tethering of CBC to the 5′ end of such a pre-mRNA rescues mRNA expression (Dower and Rosbash, 2002). Likewise, CBC is required for in vitro pre-mRNA splicing (Colot et al., 1996; Izaurralde et al., 1994; O'Mullane and Eperon, 1998). Biochemical studies identified an essen-

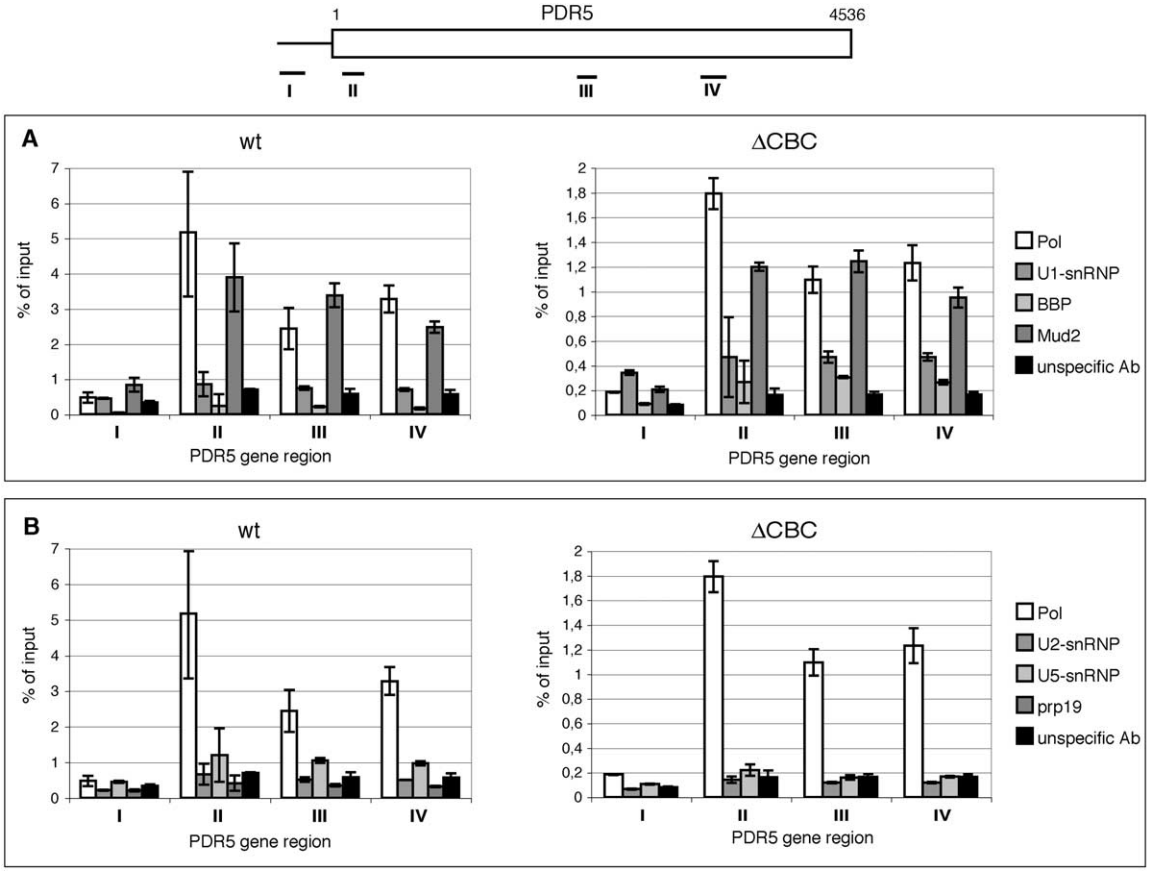

Figure 6. Mud2 Associates with the Intronless Gene *PDR5* in a CBC-Independent Manner

A diagram representing the *PDR5* gene and regions detected by PCR is shown: regions I (PCR product centered at 700 bp upstream of the ATG), II (+159 bp), III (+2323 bp), and IV (+3308 bp) are indicated.

(A) Analysis of RNA pol II and commitment complex components (the U1 snRNP, BBP, and Mud2p) in wt (left) and ΔCBC mutant strains (right). RNA pol II levels increased ~10-fold at the promoter-proximal position compared to the upstream position in both strains. The splicing factors analyzed were detected at levels near background (nonimmune IgG controls are shown), with the exception of Mud2p that increased 4- to 6-fold relative to upstream.

(B) Analysis of RNA pol II and the U2 snRNP, the U5 snRNP, and Prp19p in wt (left) and ΔCBC mutant strains (right). The data are presented as a percentage of input for each factor. For pol II and the unspecific antibody, the values from the BBP ChIP experiments were taken as representative data sets.

Error bars indicate the SD between normalized experiments. Number of independent experiments for wt and pol II, n = 4; U1 snRNP (Prp42p), n = 2; BBP, n = 4; Mud2p, n = 3; unspecific Ab, n = 4; U2 snRNP (Msl1p), n = 3; U5 snRNP (Prp8p), n = 4; and Prp19p, n = 3. For the ΔCBC mutant and pol II, n = 3; U1 snRNP (Prp42p), n = 3; BBP, n = 3; Mud2p, n = 3; unspecific Ab, n = 3; U2 snRNP (Msl1p), n = 3; and U5 snRNP (Prp8p), n = 3; Prp19p, not done.

tial role for CBC in commitment complex formation in yeast in which the U1 snRNP, BBP, and Mud2p are stably bound to the pre-mRNA and to each other through a network of interactions (Abovich and Rosbash, 1997; Colot et al., 1996; Lewis et al., 1996a). Further, the CBC was shown to facilitate U1 snRNP recruitment to the cap-proximal 5′ splice site (Lewis et al., 1996b). This evidence and the demonstration that CBC binds directly to the U1 snRNP (Fortes et al., 1999a) has led to the model that CBC stimulates splicing by promoting U1 snRNP binding to the 5′ splice site (Le Hir et al., 2003). We tested this model by examining the role of CBC in cotranscriptional commitment complex formation.

Deletion of both subunits of the CBC abolished commitment complex formation on *DBP2*. In wt strains, the U1 snRNP, BBP, and Mud2p exhibited identical patterns of accumulation that overlapped with the onset of U2 snRNP accumulation and preceded the U5 snRNP, suggesting that this transient peak represents cotranscriptional commitment complex formation. In the CBC deletion strain (Figures 4 and 7), BBP and the U1, U2, and U5 snRNPs were undetectable on *DBP2*. Interestingly, Mud2p levels and distribution along *DBP2* were identical to wt in the absence of CBC. Mud2p has been shown to bind directly to BBP and the U2 snRNP (Abovich et al., 1994; Abovich and Rosbash, 1997), and Mud2p and BBP both bind to the branchpoint (Abovich et al., 1994; Berglund et al., 1997). However, Mud2p and the branchpoint are apparently not sufficient for the recruitment of either BBP or U2 snRNP. This suggests that the primary defect in commitment complex forma-

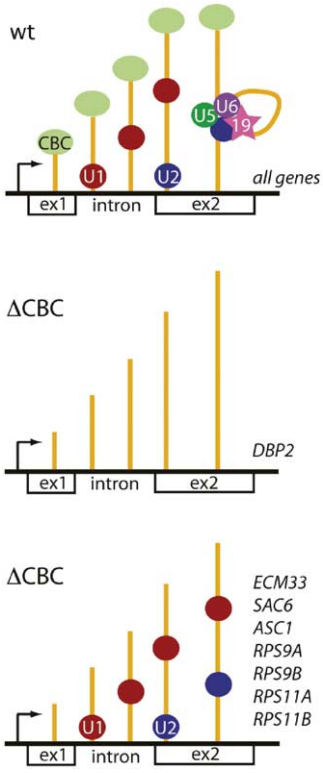

Figure 7. Schematic Diagram of Cotranscriptional Spliceosome Assembly in Wt and ΔCBC Strains

Transcription and splicing of an intron-containing gene is diagrammed, with DNA represented by black lines and nascent RNA by orange lines. In the top panel, the presence of the CBC along the transcription unit is indicated; observed accumulation patterns of U1 (red), U2 (blue), and U5 (green) snRNPs and the NTC complex (pink) are summarized, with respect to the position of 5′ and 3′ splice sites. The presence of the U6 snRNP (purple) is inferred from the detection of U5 snRNPs and the NTC (see text). The failure to assemble snRNPs on the *DBP2* gene in the absence of the CBC is shown in the middle panel. In contrast, the seven genes indicated in the bottom panel show prolonged accumulation of the U1 snRNP and failure to recruit the U5 snRNP.

tion on *DBP2* in the absence of CBC is the failure to recruit the U1 snRNP. Alternatively, a direct role for CBC in BBP recruitment is possible, and the accompanying manuscript (Lacadie and Rosbash, 2005) shows that branchpoint mutations compromise U1 snRNP recruitment.

Surprisingly, cotranscriptional commitment complex formation was unaffected by CBC deletion on *ECM33* and *SAC6*. Instead, U1 snRNP accumulation was prolonged and the U5 snRNP was nearly undetectable on these and four other genes (Figures 5 and 7). These data are reminiscent of results in HeLa nuclear extracts depleted of CBC, in which formation of early splicing complexes was normal but later steps were strongly inhibited (Izaurralde et al., 1994; O'Mullane and Eperon, 1998). Moreover, Eperon and colleagues have provided evidence that CBC actually promotes U1 snRNP removal —rather than recruitment—at some 5′ splice sites, facilitating U6 snRNA binding (O'Mullane and Eperon, 1998). It is reasonable to assume that U5 and U6 snRNP distributions are identical; therefore, these results are in complete agreement with this alternative model of CBC function. Taken together, the data verify both proposed roles of CBC: one that promotes U1 snRNP recruitment on *DBP2* and one that promotes U1 snRNP removal (Figure 7).

Current models of cotranscriptional splicing have focused on the possibility that the C-terminal domain of pol II directly binds to splicing factors and thereby promotes the efficiency of splicing (Maniatis and Reed, 2002; Zorio and Bentley, 2004). Our evidence that the CBC couples splicing to transcription raises the additional possibility that CBC directly recruits splicing factors to transcription units. If so, splicing factors may accumulate on intronless as well as intron-containing genes. In a previous study, we found that the U1 snRNP was not associated with intronless genes (Kotovic et al., 2003). Analysis of all of the splicing factors studied here on the intronless *PDR5* gene revealed that none accumulated on *PDR5*, with the exception of Mud2p, which was present on the *PDR5* promoter at levels 4-fold higher than the upstream untranscribed region. This level of association was unaffected by CBC deletion, indicating that in no case was CBC sufficient for splicing factor accumulation. Mud2p accumulation on *PDR5* may well be due to interactions with pol II (Ujvari and Luse, 2004); however, the dynamic further accumulation of Mud2p within intron-containing genes (e.g., 20-fold above upstream in *ECM33*) was not observed on *PDR5*. We propose that introns specify the dynamic accumulation of these factors, as previously reported for U1 snRNP (Kotovic et al., 2003), and that CBC plays a critical role in the progressive cotranscriptional assembly of the spliceosome.

Coupling between transcription and splicing is an important gene regulatory mechanism (Kornblihtt et al., 2004; Neugebauer, 2002; Zorio and Bentley, 2004). The unexpected finding that cotranscriptional spliceosome assembly is dependent on CBC provides a link between these processes. On the one hand, the presence of introns in a gene is known to stimulate transcription; the proximity of the 5′ splice site to the promoter is critical, and snRNPs feed back directly to the pol II elongation machinery (Fong and Zhou, 2001; Furger et al., 2002). This implies that CBC may mediate feedback from splicing to transcriptional elongation, particularly for those genes that require CBC for U1 snRNP recruitment. On the other hand, the rate of gene transcription influences alternative splice site selection, such that slowing or pausing of the polymerase increases the inclusion of weak alternative exons (de la Mata et al., 2003; Howe et al., 2003; Roberts et al., 1998). The possibility that CBC promotes cotranscriptional spliceosome assembly and thereby influences the kinetics of splice site selection is worthy of investigation. Clearly, further experiments are now necessary to determine whether the CBC also couples splicing to transcription in higher organisms.

Experimental Procedures

Yeast Strains, Growth Conditions, and Tagging

Yeast strains were grown in YPD medium, YPD plus G418 (0.2 mg/mL), synthetic complete medium plus 2% glucose without trypto-

phane, histidine, uracil, or leucine as necessary. A PCR-based strategy (Knop et al., 1999) to epitope tag endogenous genes was used to generate strains used in this study. LG1, YJV159, YJV159-ΔCBC, and MGD353-13D were used as parental strains. YJV159 and YJV159-ΔCBC strains (Fortes et al., 1999b) were generous gifts of Iain Mattaj. Different wt strains showed the same accumulation of factors on the genes analyzed. All primers used in this study were obtained from SIGMA Genosys. Primer sequences and strain information are available upon request. Complementation of the ΔCBC phenotype by galactose-induced expression of CBP80 and CBP20 was accomplished by cloning CBP20 and CBP80 cDNAs from the wt strain LG1 into the p415GAL1 and p416GAL1 vectors. Tagged ΔCBC strains were double transformed with the two expression vectors and selected. Positive clones were grown in SD-Leu-Ura medium with 2% raffinose and then resuspended in medium with 2% galactose for 6 hr.

ChIP and Quantitative Real-Time PCR

ChIP was performed as described (Kotovic et al., 2003). Anti-HA mAb 12CA5 (Roche) for HA-tagged proteins, anti-myc mAb 9E10 (Santa Cruz) for myc-tagged proteins, and mAb 8WG16 (Babco) against RNA pol II were used, followed by GammaBind Sepharose beads (Amersham). Nonimmune mouse IgG (Sigma) was used as a negative control.

DNA templates retrieved by ChIP were analyzed by quantitative real-time PCR (Q-PCR) using the SYBR Green method (absolute SYBR Green ROX Mix, ABGene) and a Stratagene MX3000. The reaction volume was 10 μl, with 1 μl template (supernatant 1:10 diluted) and 100–300 nM of each primer according to individual optimization. Cycling was done for 15 min at 95°C, followed by 40 cycles for 30 s at 95°C, 1 min at 59°C, and 30 s at 72°C, with measuring at the end of the 59°C step. Dissociation curves were obtained by heating samples to 95°C, followed by cooling down to 55°C and successive heating of the samples to 95°C with continuous measurement. Primer sets distinguished between different regions of the genes tested, with PCR products indicated relative to ATG as follows: *DBP2* and *DBP2-GFP*: 153–210, 521–653, 667–815, 863–929, 1457–1528, 1736–1852, 2379–2522, and 2730–2872; *ECM33*: −589–(−492), −2–(+134), 419–551, 1073–1174, 1296–1398, and 1520–1572; *SAC6*: −203–(−141), 246–335, 558–614, and 1287–1387; and *PDR5*: −755–(−667), 122–196, 2273–2373, and 3279–3357. Data sets were normalized to ChIP input values, then the values for the DNA obtained with the unspecific antibody were subtracted from values for pol II and the splicing factor analyzed ($2^{Ct(spec)-Ct(input)} - 2^{Ct(unspec)-Ct(input)}$). See figure legends for further details.

Supplemental Data

Supplemental Data include one table and are available with this article online at http://www.molecule.org/cgi/content/full/19/1/53/DC1/.

Acknowledgments

We thank Iain Mattaj for generously providing the ΔCBP20-ΔCBP80 strain. We are grateful to members of our laboratory, Bertrand Seraphin, Michael Rosbash, and Scott Lacadie for helpful discussions and comments on the manuscript. This research was funded by support from the Max Planck Gesellschaft.

Received: January 28, 2005
Revised: April 5, 2005
Accepted: May 9, 2005
Published: June 30, 2005

References

Abovich, N., and Rosbash, M. (1997). Cross-intron bridging interactions in the yeast commitment complex are conserved in mammals. Cell *89*, 403–412.

Abovich, N., Liao, X.C., and Rosbash, M. (1994). The yeast MUD2 protein: an interaction with PRP11 defines a bridge between commitment complexes and U2 snRNP addition. Genes Dev. *8*, 843–854.

Azubel, M., Wolf, S.G., Sperling, J., and Sperling, R. (2004). Three-dimensional structure of the native spliceosome by cryo-electron microscopy. Mol. Cell *15*, 833–839.

Berglund, J.A., Chua, K., Abovich, N., Reed, R., and Rosbash, M. (1997). The splicing factor BBP interacts specifically with the pre-mRNA branchpoint sequence UACUAAC. Cell *89*, 781–787.

Beyer, A.L., and Osheim, Y.N. (1988). Splice site selection, rate of splicing, and alternative splicing on nascent transcripts. Genes Dev. *2*, 754–765.

Blanchette, M., Labourier, E., Green, R.E., Brenner, S.E., and Rio, D.C. (2004). Genome-wide analysis reveals an unexpected function for the Drosophila splicing factor U2AF(50) in the nuclear export of intronless mRNAs. Mol. Cell *14*, 775–786.

Burckin, T., Nagel, R., Mandel-Gutfreund, Y., Shiue, L., Clark, T.A., Chong, J.L., Chang, T.H., Squazzo, S., Hartzog, G., and Ares, M., Jr. (2005). Exploring functional relationships between components of the gene expression machinery. Nat. Struct. Mol. Biol. *12*, 175–182.

Chan, S.P., Kao, D.I., Tsai, W.Y., and Cheng, S.C. (2003). The Prp19p-associated complex in spliceosome activation. Science *302*, 279–282.

Chen, J.Y., Stands, L., Staley, J.P., Jackups, R.R., Jr., Latus, L.J., and Chang, T.H. (2001). Specific alterations of U1-C protein or U1 small nuclear RNA can eliminate the requirement of Prp28p, an essential DEAD box splicing factor. Mol. Cell *7*, 227–232.

Chiara, M.D., Gozani, O., Bennett, M., Champion-Arnaud, P., Palandjian, L., and Reed, R. (1996). Identification of proteins that interact with exon sequences, splice sites, and the branchpoint sequence during each stage of spliceosome assembly. Mol. Cell. Biol. *16*, 3317–3326.

Colot, H.V., Stutz, F., and Rosbash, M. (1996). The yeast splicing factor Mud13p is a commitment complex component and corresponds to CBP20, the small subunit of the nuclear cap-binding complex. Genes Dev. *10*, 1699–1708.

de la Mata, M., Alonso, C.R., Kadener, S., Fededa, J.P., Blaustein, M., Pelisch, F., Cramer, P., Bentley, D., and Kornblihtt, A.R. (2003). A slow RNA polymerase II affects alternative splicing in vivo. Mol. Cell *12*, 525–532.

Dower, K., and Rosbash, M. (2002). T7 RNA polymerase-directed transcripts are processed in yeast and link 3′ end formation to mRNA nuclear export. RNA *8*, 686–697.

Elliott, D.J., and Rosbash, M. (1996). Yeast pre-mRNA is composed of two populations with distinct kinetic properties. Exp. Cell Res. *229*, 181–188.

Fong, Y.W., and Zhou, Q. (2001). Stimulatory effect of splicing factors on transcriptional elongation. Nature *414*, 929–933.

Fortes, P., Bilbao-Cortes, D., Fornerod, M., Rigaut, G., Raymond, W., Seraphin, B., and Mattaj, I.W. (1999a). Luc7p, a novel yeast U1 snRNP protein with a role in 5′ splice site recognition. Genes Dev. *13*, 2425–2438.

Fortes, P., Kufel, J., Fornerod, M., Polycarpou-Schwarz, M., Lafontaine, D., Tollervey, D., and Mattaj, I.W. (1999b). Genetic and physical interactions involving the yeast nuclear cap-binding complex. Mol. Cell. Biol. *19*, 6543–6553.

Fresco, L.D., and Buratowski, S. (1996). Conditional mutants of the yeast mRNA capping enzyme show that the cap enhances, but is not required for, mRNA splicing. RNA *2*, 584–596.

Furger, A., O'Sullivan, J.M., Binnie, A., Lee, B.A., and Proudfoot, N.J. (2002). Promoter proximal splice sites enhance transcription. Genes Dev. *16*, 2792–2799.

Howe, K.J., Kane, C.M., and Ares, M., Jr. (2003). Perturbation of transcription elongation influences the fidelity of internal exon inclusion in Saccharomyces cerevisiae. RNA *9*, 993–1006.

Izaurralde, E., Lewis, J., McGuigan, C., Jankowska, M., Darzynkiewicz, E., and Mattaj, I.W. (1994). A nuclear cap binding protein complex involved in pre-mRNA splicing. Cell *78*, 657–668.

Jurica, M.S., and Moore, M.J. (2003). Pre-mRNA splicing: awash in a sea of proteins. Mol. Cell *12*, 5–14.

Jurica, M.S., Licklider, L.J., Gygi, S.R., Grigorieff, N., and Moore, M.J. (2002). Purification and characterization of native spliceosomes suitable for three-dimensional structural analysis. RNA *8*, 426–439.

Knop, M., Siegers, K., Pereira, G., Zachariae, W., Winsor, B., Nasmyth, K., and Schiebel, E. (1999). Epitope tagging of yeast genes using a PCR-based strategy: more tags and improved practical routines. Yeast *15*, 963–972.

Konforti, B.B., Koziolkiewicz, M.J., and Konarska, M.M. (1993). Disruption of base pairing between the 5′ splice site and the 5′ end of U1 snRNA is required for spliceosome assembly. Cell *75*, 863–873.

Kornblihtt, A.R., de la Mata, M., Fededa, J.P., Munoz, M.J., and Nogues, G. (2004). Multiple links between transcription and splicing. RNA *10*, 1489–1498.

Kotovic, K.M., Lockshon, D., Boric, L., and Neugebauer, K.M. (2003). Cotranscriptional recruitment of the U1 snRNP to intron-containing genes in yeast. Mol. Cell. Biol. *23*, 5768–5779.

Lacadie, S.A., and Rosbash, M. (2005). Cotranscriptional spliceosome assembly dynamics and the role of U1 snRNA:5′ss base pairing in yeast. Mol. Cell *19*, this issue, 65–75.

Le Hir, H., Nott, A., and Moore, M.J. (2003). How introns influence and enhance eukaryotic gene expression. Trends Biochem. Sci. *28*, 215–220.

Lewis, J.D., Gorlich, D., and Mattaj, I.W. (1996a). A yeast cap binding protein complex (yCBC) acts at an early step in pre- mRNA splicing. Nucleic Acids Res. *24*, 3332–3336.

Lewis, J.D., Izaurralde, E., Jarmolowski, A., McGuigan, C., and Mattaj, I.W. (1996b). A nuclear cap-binding complex facilitates association of U1 snRNP with the cap-proximal 5′ splice site. Genes Dev. *10*, 1683–1698.

Makarov, E.M., Makarova, O.V., Urlaub, H., Gentzel, M., Will, C.L., Wilm, M., and Luhrmann, R. (2002). Small nuclear ribonucleoprotein remodeling during catalytic activation of the spliceosome. Science *298*, 2205–2208.

Makarova, O.V., Makarov, E.M., Urlaub, H., Will, C.L., Gentzel, M., Wilm, M., and Luhrmann, R. (2004). A subset of human 35S U5 proteins, including Prp19, function prior to catalytic step 1 of splicing. EMBO J. *23*, 2381–2391.

Malca, H., Shomron, N., and Ast, G. (2003). The U1 snRNP base pairs with the 5′ splice site within a penta-snRNP complex. Mol. Cell. Biol. *23*, 3442–3455.

Maniatis, T., and Reed, R. (2002). An extensive network of coupling among gene expression machines. Nature *416*, 499–506.

Maroney, P.A., Romfo, C.M., and Nilsen, T.W. (2000). Functional recognition of 5′ splice site by U4/U6.U5 tri-snRNP defines a novel ATP-dependent step in early spliceosome assembly. Mol. Cell *6*, 317–328.

Michaud, S., and Reed, R. (1991). An ATP-independent complex commits pre-mRNA to the mammalian spliceosome assembly pathway. Genes Dev. *5*, 2534–2546.

Miriami, E., Angenitzki, M., Sperling, R., and Sperling, J. (1995). Magnesium cations are required for the association of U small nuclear ribonucleoproteins and SR proteins with pre-mRNA in 200 S large nuclear ribonucleoprotein particles. J. Mol. Biol. *246*, 254–263.

Neugebauer, K.M. (2002). On the importance of being co-transcriptional. J. Cell Sci. *115*, 3865–3871.

Nilsen, T.W. (2002). The spliceosome: no assembly required? Mol. Cell *9*, 8–9.

Nilsen, T.W. (2003). The spliceosome: the most complex macromolecular machine in the cell? Bioessays *25*, 1147–1149.

O'Mullane, L., and Eperon, I.C. (1998). The pre-mRNA 5′ cap determines whether U6 small nuclear RNA succeeds U1 small nuclear ribonucleoprotein particle at 5′ splice sites. Mol. Cell. Biol. *18*, 7510–7520.

Ohi, M.D., Vander Kooi, C.W., Rosenberg, J.A., Ren, L., Hirsch, J.P., Chazin, W.J., Walz, T., and Gould, K.L. (2005). Structural and functional analysis of essential pre-mRNA splicing factor Prp19p. Mol. Cell. Biol. *25*, 451–460.

Orlando, V. (2000). Mapping chromosomal proteins in vivo by formaldehyde-crosslinked-chromatin immunoprecipitation. Trends Biochem. Sci. *25*, 99–104.

Raitskin, O., Angenitzki, M., Sperling, J., and Sperling, R. (2002). Large nuclear RNP particles—the nuclear pre-mRNA processing machine. J. Struct. Biol. *140*, 123–130.

Rappsilber, J., Ryder, U., Lamond, A.I., and Mann, M. (2002). Large-scale proteomic analysis of the human spliceosome. Genome Res. *12*, 1231–1245.

Reed, R. (2000). Mechanisms of fidelity in pre-mRNA splicing. Curr. Opin. Cell Biol. *12*, 340–345.

Roberts, G.C., Gooding, C., Mak, H.Y., Proudfoot, N.J., and Smith, C.W. (1998). Co-transcriptional commitment to alternative splice site selection. Nucleic Acids Res. *26*, 5568–5572.

Schwer, B., and Shuman, S. (1996). Conditional inactivation of mRNA capping enzyme affects yeast pre-mRNA splicing in vivo. RNA *2*, 574–583.

Seraphin, B., and Rosbash, M. (1989). Identification of functional U1 snRNA-pre-mRNA complexes committed to spliceosome assembly and splicing. Cell *59*, 349–358.

Shuman, S. (2001). Structure, mechanism, and evolution of the mRNA capping apparatus. Prog. Nucleic Acid Res. Mol. Biol. *66*, 1–40.

Staley, J.P., and Guthrie, C. (1998). Mechanical devices of the spliceosome: motors, clocks, springs, and things. Cell *92*, 315–326.

Stevens, S.W., Ryan, D.E., Ge, H.Y., Moore, R.E., Young, M.K., Lee, T.D., and Abelson, J. (2002). Composition and functional characterization of the yeast spliceosomal penta-snRNP. Mol. Cell *9*, 31–44.

Tarn, W.Y., Hsu, C.H., Huang, K.T., Chen, H.R., Kao, H.Y., Lee, K.R., and Cheng, S.C. (1994). Functional association of essential splicing factor(s) with PRP19 in a protein complex. EMBO J. *13*, 2421–2431.

Ujvari, A., and Luse, D.S. (2004). Newly Initiated RNA encounters a factor involved in splicing immediately upon emerging from within RNA polymerase II. J. Biol. Chem. *279*, 49773–49779.

Visa, N., Izaurralde, E., Ferreira, J., Daneholt, B., and Mattaj, I.W. (1996). A nuclear cap-binding complex binds Balbiani ring pre-mRNA cotranscriptionally and accompanies the ribonucleoprotein particle during nuclear export. J. Cell Biol. *133*, 5–14.

Wetterberg, I., Zhao, J., Masich, S., Wieslander, L., and Skoglund, U. (2001). In situ transcription and splicing in the Balbiani ring 3 gene. EMBO J. *20*, 2564–2574.

Wyatt, J.R., Sontheimer, E.J., and Steitz, J.A. (1992). Site-specific cross-linking of mammalian U5 snRNP to the 5′ splice site before the first step of pre-mRNA splicing. Genes Dev. *6*, 2542–2553.

Zenklusen, D., Vinciguerra, P., Wyss, J.C., and Stutz, F. (2002). Stable mRNP formation and export require cotranscriptional recruitment of the mRNA export factors Yra1p and Sub2p by Hpr1p. Mol. Cell. Biol. *22*, 8241–8253.

Zhou, Z., Licklider, L.J., Gygi, S.P., and Reed, R. (2002). Comprehensive proteomic analysis of the human spliceosome. Nature *419*, 182–185.

Zorio, D.A., and Bentley, D.L. (2004). The link between mRNA processing and transcription: communication works both ways. Exp. Cell Res. *296*, 91–97.